International Journal of Applied Science and Engineering

Impact of diameter to thickness (D/t) on axial capacity of circular CFST columns: Experimental, parametric and numerical analysis

Shaik Madeena Imam Shah, G. Mohan Ganesh*

School of Civil Engineering, Vellore Institute of Technology, Vellore 632014, Tamil Nadu, India

ABSTRACT

Twenty-four circular Concrete Filled Steel Tube (CFST) columns divided in to three series based on their cross-sectional dimensions were subjected to uni-axial compression and their behaviour is studied. This paper aims to develop the volume of experimental database as there is shortage in data that can assess the guidance from the codes and enhances their accuracy in determining the ultimate capacities and the behaviour of CFST specimens subjected to uni axial compression. This study consists of CFST specimens having outer diameter of 76 mm, 89 mm and 100 mm with same wall thickness of 3 mm having four Length to Diameter (L/D) ratios of 3, 4, 5 and 6. Impact of D/t on the parameters like confinement (ξ), strength index (SI), relative slenderness ratio (λ), percentage contribution of steel and concrete and ductility index (DI) were studied. Further, the axial compressive load values were compared with the predicted design values of codes, namely, Eurocode – 4 (EC4), American code (AISC 360-10), Australian code (AS5100), Chinese code (DBJ13-51) and American Concrete Institute (ACI-318). A design equation is proposed to calculate the ultimate axial load and the predicted results are near to the test results. To check the accuracy of the proposed equation, experimental results of 63 CFST circular columns from the literatures were compared with proposed equation and found the results to be conservative. At last, finite element analysis using ABAQUS was done to study the behaviour of column buckling, axial load and displacement curves. Results showed good agreement with experimental test results.

Keywords: Concrete contribution ratio, Ductility index, Length to diameter, Overestimated, Underestimated.

OPEN ACCESS

Received: November 10, 2021
Revised: February 14, 2022
Accepted: March 23, 2022

Corresponding Author:
G. Mohan Ganesh
gmohanganesh@vit.ac.in

Publisher:
Chaoyang University of Technology
ISSN: 1727-2394 (Print)
ISSN: 1727-7841 (Online)

1. INTRODUCTION

Concrete Filled Steel Tube (CFST) columns having the advantage of exceptional axial carrying capacity are used in modern developments of structures like bridges with long span, high rise buildings, subways, transmitting poles and other infrastructures (Feng et al., 2020). As the demand of economy is high and constructions are rapid, CFST columns have come in to play with practical applications. SEG Plaza in Shenzhen – China is one of the first structures using circular concrete filled steel tube columns in a very large scale. The diameter of circular CFST used in this construction ranged from 900 mm to 1600 mm (Zhao et al., 2010). Also, Obayshi Technical Research Institute is constructed using circular CFST columns having steel grade of 780 MPa and columns in Tokyo Sky Tree has the steel grade of 700 MPa. Both the structures are constructed in Japan. The diameters of the columns used in the structure ranged from 2000 mm to 2300 mm (Li et al., 2020). Canton Tower in China topped out in the year 2009 and opened in 2010 which has 604 m height used circular CFST columns having diameter about 3200 mm. All these structures mentioned above are beyond the limit of substantial design codes such as AS5100, EC4, DBJ13-51 and AISC. The parameters in these design codes

were limited to certain ranges because of its early research developments and their results. The design capacities and parametric limits of these codes are represented in Table 1.

Research and experimental work have been conducted on CFST columns having yield strength, high strength concrete and different diameter to thickness ratios. Dundu (2012) studied the behaviour of 24 CFST columns having diameter ranging from 114.85 mm to 193.7 mm with a thickness of 3 – 3.5 mm. Yield strength of steel and concrete strength considered was 345 – 488 MPa and 30-40.3 MPa respectively. Author has concluded that, columns with higher diameter and hoop stress results in increasing the load carrying capacity. The experimental results are 8.4% and 13.6% conservative with the predicted values of EC4 codes respectively. Wang et al. (2017) studied the effect of size in circular CFST with different D/t ratios ranging from 55 - 88 under axial compression and concluded that effect of size has more impact on the columns.

Ekmekyapar et al. (2016) presented 18 CFST circular columns of various lengths having concrete grade strength between 50 MPa to 110 MPa with diameter of 114.3 mm and thickness ranging from 2.74 to 5.9 mm. It is concluded that, EC4 had better acceptance with the test results and suggested to widen the range of limits for better research and experimental works. Zeghiche et al. (2005) tested 27 CFST specimens with f_c = 40 MPa to 106 MPa, having diameter ranging from 159-160 mm and thickness of 4.9 – 5.13 mm.

Table 1. Code specifications and limits

Code	D/t Limit	Steel yield strength	Concrete strength	Relative slenderness ratio	Axial capacity prediction
EC4	$90(\frac{235}{f_y})$	$235 \le f_y \le 460$	$20 \le f_c \le 60$	$\lambda = \sqrt{\frac{N_{pl,Rk}}{N_{cr}}} \le 2.0$ $N_{pl,Rk} = A_s f_y + A_c f_c$ $N_{cr} = \frac{\pi^2 (EI)_{eff}}{(L)^2}$ $(EI)_{eff} = E_s I_s + 0.6 E_c I_c$	$N_u = A_s \eta_a f_y + A_c f_c \left(1 + \eta_c \frac{t}{d} \frac{f_y}{f_c}\right)$ $\eta_a = 0.25 (3 + 2\lambda) \le 1.0$ $\eta_c = 4.9 - 18.5 \lambda + 17 \lambda^2 \ge 0$
AS 5100	$90(\frac{235}{f_y})$	$200 \le f_y \le 450$	$25 \le f_c \le 65$	$\lambda = \sqrt{\frac{N_s}{N_{cr}}} \le 2.0$ $N_s = A_s f_y + A_c f_c$ $N_{cr} = \frac{\pi^2 (EI)_e}{(L)^2}$ $(EI)_e = \phi E_s I_s + \phi_c E_c I_c$	$N_u = \phi A_s \eta_2 f_y + \phi_c A_c f_c \left(1 + \eta_1 \frac{t}{d} \frac{f_y}{f_c}\right)$ $\eta_1 = 4.9 - 18.5 \lambda_r + 17 \lambda^2 \ge 0$ $\eta_2 = 0.25 (3 + 2\lambda) \le 1.0$ $\emptyset = 0.9, \emptyset_c = 0.6$
DBJ 13-51	$150 (\frac{235}{f_y})$	$235 \le f_y \le 420$	$20 \le f_c \le 50$	- $\xi = \frac{A_s f_y}{A_c f_c}$	$N_u = f_{sc} A_{sc}$ $A_{sc} = A_s + A_c$ $f_{sc} = (1.14 + 1.02 \xi). f_c$
AISC 360-10	$\lambda_p = 0.15 \frac{E_s}{f_y}$ $\lambda_r = 0.19 \frac{E_s}{f_y}$	$f_y \le 525$	$21 \le f_c \le 70$	-	$P_n = P_{no}[0.658^{\frac{P_{no}}{P_e}}]$ $\frac{P_{no}}{P_e} \le 2.25$ $P_n = 0.877 P_e$ $\frac{P_{no}}{P_e} > 2.25$ $P_{no} = P_p = A_s f_y + 0.95 A_c f_c$ $\frac{D}{t} < \lambda_p$ $P_{no} = P_p - \frac{P_p - P_y}{(\lambda_r - \lambda_p)^2} (\lambda - \lambda_p)^2$ $\lambda_p < \frac{D}{t} < \lambda_r$ $P_y = A_s f_y + 0.7 A_c f_c$ $P_{no} = A_s f_{cr} + 0.7 A_c f_c$ $f_{cr} = \frac{0.72 f_y}{((\frac{D}{t})\frac{f_y}{E_s})^{0.2}}$
ACI-318	-	-	-	-	$P_{ACI} = 0.85 f_c A_c + f_y A_s$

It is concluded that concrete having high strength intensified the column axial capacity and EC4 predictions are safe and in good accord with experimental and numerical failure loads. Similarly, Ou et al. (2011) conducted experimental study having the diameter range from 222-488 mm with steel tube thickness of 1.5 mm, all the 27 specimens used in the study had their D/t limit beyond the code provisions. The conclusions given by the author is that as eccentricity and slenderness are increasing, the load capacity of the CFST columns is decreasing. Fang and Visintin (2021) studied the structural performance of 6 square and 5 circular geopolymer CFST members having B x t of 125 x 4 mm and D x t of 140 x 3.6 mm respectively. All the specimens were subjected to compression and flexural bending. It is concluded here that, ultimate load of the specimen decreased with increasing eccentric loading. Greater structural performance can be obtained with lesser B/t or D/t and member slenderness ratios. Authors also compared the experimental test results with design codes like EC4, AS/NZS2327 and AISC 360 and concluded that these codes are safe to apply in generating the design of geopolymer CFST members. Dar et al. (2021) studied the axial strength and deformation behaviour of light weight CFS composite built up columns that are formed using GFRP and timber and showed that the axial strength improvement in the short CFS composite columns due to double GFRP is very near to that of GFRP sheets and timber plank. Many researchers have studied the axial compressive behaviour of CFST columns and disclosed that, as the length of columns are increasing, the axial capacities are decreasing. The effect of length (L) on CFST axial capacity also differs among various design codes. EC4 and AS5100 has similar approach on the design of predicting the capacity of the column, where it introduces an effective length factor (k) with idealized end restraints. While the approach in AISC is based on Euler's formula that considers the effect of slenderness ratio. DBJ13-51 has completely different approach in predicting the capacity and there is no such parameter length (L) that influences the axial capacity. Confinement factor (ξ) is the main parameter that influences the axial capacity of the column. Based on the literature review, enormous data shows that materials are within and beyond the limit of application in design codes that effect the axial capacity of the columns. Hence, the study of parameters and size effect of column enhances the design specifications and allows to revise the method of approach in predicting the axial capacities. This paper shows the experimental behaviour and parametric analysis of CFST columns having different diameter to thickness and length to diameter ratios. In addition, the experimental results are compared to the predicted code results. The design codes used in this study are Eurocode-4(EC4), American code (AISC360-10), Australian code (AS5100), Chinese code (DBJ13-51) and American Concrete Institute (ACI - 318). The main aim of this study is to enhance the data of experimental study available with current series of test data on CFST columns under uni axial compression.

2. EXPERIMENTAL STRATEGY

2.1 Test Setup and Details

24 CFST columns having outer diameter of 76 mm, 89 mm and 100 mm with same wall thickness of 3 mm were taken for the experimental study. The specimens were divided in to three series depending on their cross-sectional dimension. Each series had 8 specimens of L/D ratio of 3, 4, 5 and 6. For each L/D ratio, two specimens were cast, exhibited for axial load compression and the average load of the two specimens were recorded. Similarly, all the series had 8 specimens of L/D ratio 3, 4, 5 and 6 and two specimens for each L/D were cast and tested in UTM recording the average ultimate load of the specimens. In order to have ease, the series were named as follows: OD76-3t, OD89-3t and OD100-3t in which, 'OD' and 't' represents outer diameter and thickness respectively. The experimental work was completely carried out at VIT University – Vellore (India). The reason for choosing the small diameters was to study the behaviour of columns that has the load carrying capacity below 1000 kN. The available diameters from the market were chosen for the research study as the UTM had the limited capacity of 1000 kN. Fig. 1 shows the specimen placed in UTM with a dial gauge fixed beside the specimen for recording the axial deformation values.

Fig. 1. Specimen placed in UTM for testing

2.2 Properties of Materials

2.2.1 Steel Tubes

Hot rolled steel tubes were fabricated and supplied by the manufacturer available locally. Coupon test was conducted to find out the elastic modulus of the steel plate specimen which was used to fabricate the CFST columns and found the value to be 208.4 GPa, which is in the prescribed limits of steel yield strength as shown from Table 1. Steel columns had outer diameter of 76 mm, 89 mm and 100 mm with a wall thickness of 3 mm were used in the experimental study.

2.2.2 Concrete

In this study, self-compacting concrete (SCC) having M30 grade which satisfied all the prescribed mandates by the EFNARC code was used as infill in the steel hollow columns. Poly carboxylate ether (PCE) based super plasticizer named MasterGlenium SKY 8233 having pH value greater than 6 and specific gravity of 1.08 was used to obtain the mix. SCC has satisfied all the basic fresh properties like slump flow and V-Funnel. The mix proportion, limits and values of the fresh properties are summarised in Table 2. Aligned with the CFST experimental work, compressive strength of concrete (f_c) was carried out in 150 x 150 x 150 mm cubes. Three concrete sample cubes were cast and placed in curing tank for 28 days and the final recorded compressive strength is given in Table 3. The process of filling the concrete was so easy because it had self-flow and vibration was not necessary. The base of the hollow column was attached to a plate and the concrete was filled. All the specimens were machined to achieve smooth base in the top and bottom and painted to avoid corrosion before placing into the curing tank. Fig 2 shows the cross-sectional dimensions of the specimens that were ready for testing.

3. EXPERIMENTAL APPROACH AND RESULTS

All the CFST specimens were subjected to uni-axial compression till failure. Columns were placed vertically in UTM with the base plates at the top and bottom to have the uniform loading on steel and concrete (Fig.1). Axial load was applied 2 mm per minute to control correctly and record the experimental results accurately. After reaching the failure load, the experiment was continued till the specimen reached 85% of its peak load in order to study the ductility behaviour of the columns.

3.1 Test Results

Failure modes of each specimen was captured and registered safely. Fig. 3 shows the specimens failed after testing. The behaviour of each specimen can be represented through the load verses deflection curves for various L/D ratios for series 1, 2 and 3 as shown in Fig. 4.

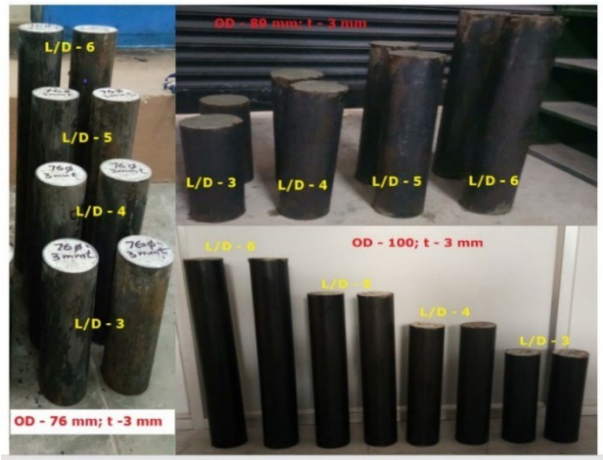

Fig. 2. CFST specimens with cross sectional details

Table 2. Mix proportions and fresh properties

Cement (kg/m^3)	Fine aggregate (kg/m^3)	Coarse aggregate (kg/m^3)	Water-cement ratio	Super plasticizer (%)	Slump flow (mm)	V-Funnel (sec)
450	740	810	0.46	0.85	610	06

Fig. 3. Failure mode of specimens

In general, the specimens in all the series failed due to outward buckling of steel tube, while local bucking was observed at the mid length of the sections. Circular specimens with larger diameter and lesser L/D ratio exhibited more ductile behaviour compared to larger L/D ratios. The columns with increasing L/D ratios, showed decreasing axial compressive capacity. The values of the column capacities are summarized in Table 3. As per the ductile performance of the specimens are concerned, relatively low ductility is seen in the specimens with lesser diameter. This effect is inverse as the length is increasing. It is as expected that the capacity of the column is higher for specimens having larger area of steel and concrete.

3.2 D/T and L/D of the Columns

Fig. 5 shows the graph plotted between L/D and axial load of the CFST column for all the series of the specimens. Since yield strength, compressive strength and thickness of the specimens are same in all the series, the effect in axial load is influenced by the diameter of the column. It can be seen from the graph that, series 3 that is OD100-3t have higher axial capacities compared to other two series of specimens. However, the axial load decreased as the L/D of the column increased which is as expected.

Series 3 which is OD100-3t having L/D ratio 3 showed 7.24% increment compared to column having L/D ratio 6. 3.66% and 0.33% increment compared to columns with L/D ratios 5 and 4 respectively.

Specimens with L/D ratio 3 in OD100-3t (series 3) showed an increment of 13.41% compared to OD89-3t (series 2) having L/D ratio of 3 and 39.45% compared to OD76-3t having L/D ratio 3. It is inferred here that, as the yield strength and thickness of the columns are same for all the specimens, influence of diameter on axial capacity of column is predominant.

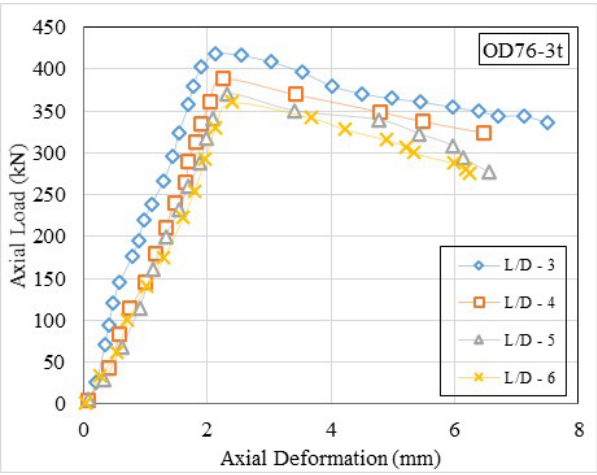

(a) Series 1

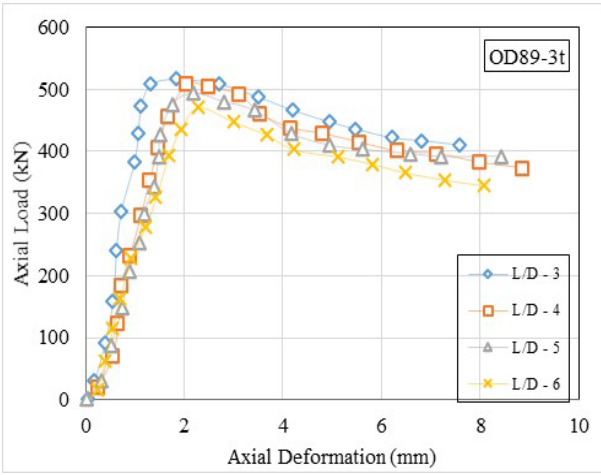

(b) Series 2

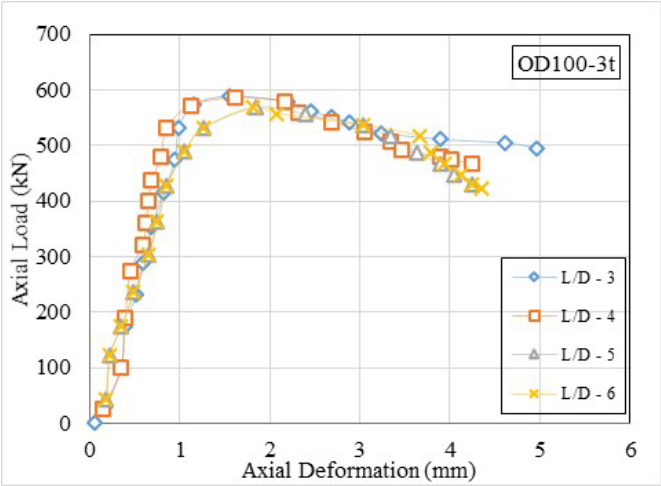

(c) Series 3

Fig. 4. Axial load versus axial deformation curves for all the series of CFST specimens

3.3 Confinement Effect

As the yield strength and concrete strength of all the specimens are same, the confinement effect depends on the cross-section area of steel and concrete which differs with the diameter of the column. Confinement (ξ) is calculated using the expression given in Table 1 in DBJ13-51 section. Fig. 6 shows the plot between D/t and confinement (ξ). As the D/t of the column is increasing, the confinement effect is decreasing.

Also, confinement (ξ) has much influence on the axial capacity of the column which can be seen from Fig. 7. The axial capacity of the column increases with the increase in the cross-sectional area of steel and concrete which is the main parameter that influences the confinement (ξ). However, L/D has inverse effect on the load carrying capacity.

Table 3. Column details are test results

Series and Title		L/D	f_y (MPa)	f_c (MPa)	A_s (mm^2)	A_c (mm^2)	N_e (kN)	P_s%	P_c%	λ	ξ	SI	δ (mm)	DI
1	OD76-3t	3	255	38.6	688.01	3848.4	424.5	41.3	58.6	0.118	1.181	1.405	2.16	2.54
	OD76-3t	4	255	38.6	688.01	3848.4	394	44.5	55.4	0.158	1.181	1.313	2.27	1.46
	OD76-3t	5	255	38.6	688.01	3848.4	376.5	46.6	53.4	0.197	1.181	1.256	2.32	1.51
	OD76-3t	6	255	38.6	688.01	3848.4	364.5	48.1	51.8	0.237	1.181	1.193	2.41	1.60
2	OD89-3t	3	255	38.6	862.55	5358.6	522	42.1	57.8	0.119	1.063	1.319	1.84	2.68
	OD89-3t	4	255	38.6	862.55	5358.6	516	42.7	57.2	0.159	1.063	1.299	2.04	2.02
	OD89-3t	5	255	38.6	862.55	5358.6	496	44.3	55.6	0.199	1.063	1.253	2.19	1.90
	OD89-3t	6	255	38.6	862.55	5358.6	479	45.9	54.0	0.239	1.063	1.210	2.31	1.84
3	OD100-3t	3	255	38.6	914.2	6939.7	592	39.3	60.6	0.122	0.870	1.285	1.56	2.96
	OD100-3t	4	255	38.6	914.2	6939.7	590	39.5	60.4	0.162	0.870	1.280	1.62	2.14
	OD100-3t	5	255	38.6	914.2	6939.7	572	40.8	59.1	0.203	0.870	1.239	1.82	1.97
	OD100-3t	6	255	38.6	914.2	6939.7	550	42.2	57.7	0.244	0.870	1.198	2.09	1.89

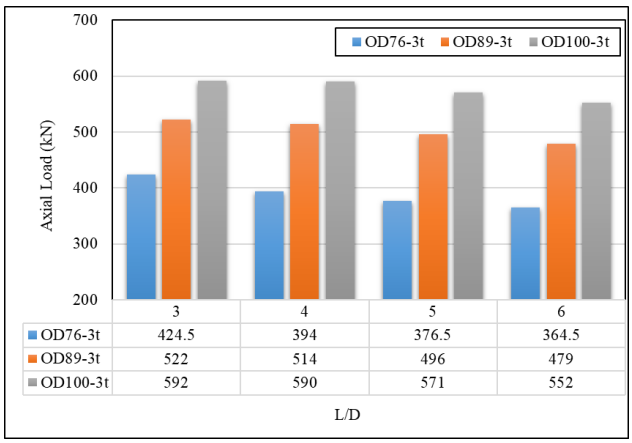

Fig. 5. Axial capacities of CFST columns of various diameters

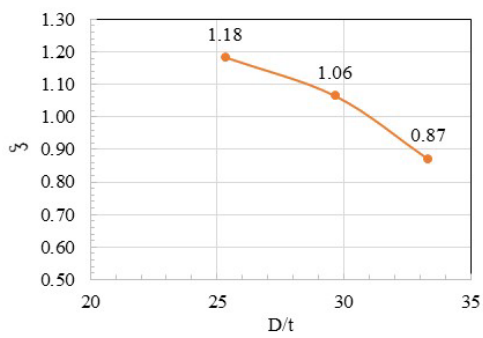

Fig. 6. D/t versus confinement effect

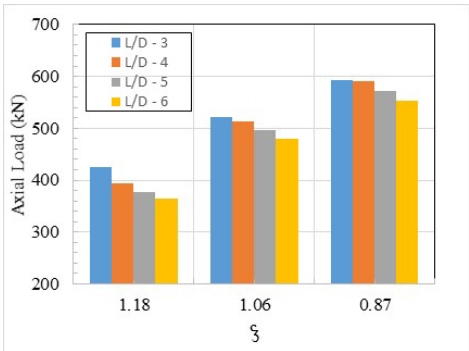

Fig. 7. Effect of confinement on axial capacities of the columns

3.4 Strength Index

Strength Index (SI) is an important parameter that is used to measure the composite action between concrete core and steel tube. It is also used to analyse the performance of columns. Equation of SI is as follows:

$$SI = \frac{N_u}{A_s f_y + A_c f_c} \quad (1)$$

where N_u is ultimate axial capacity of the composite specimen governed either by experimental data or design code value. The denominator specifies the squash load of the specimen. Where A_s and f_y are cross sectional area and yield strength of the steel tube respectively. A_c and f_c are cross sectional area and concrete compressive strength respectively. The strength index values are given in Table 3.

The values of SI for series 1 (OD76-3t) ranges from 1.405 to 1.193 while the values of other two series (OD89-3t and OD100-3t) varies from 1.319 to 1.210 and 1.285 to 1.198. Fig. 8 and 9 shows the plot between SI versus L/D and SI versus confinement (ξ) respectively. It can be observed that a general increment of L/D leads to decrease in SI. However, increase in size of diameter will increase the cross-sectional area of steel tube thereby decreases the confinement which also leads to low performance in strength index of the column. The reduction in axial capacities of CFST specimens may occur due to global imperfections.

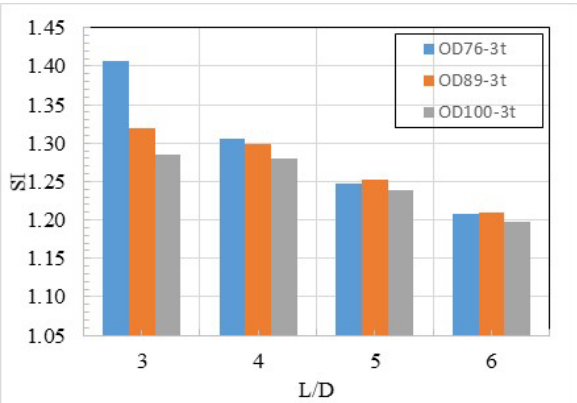

Fig. 8. Strength index versus L/D of the columns

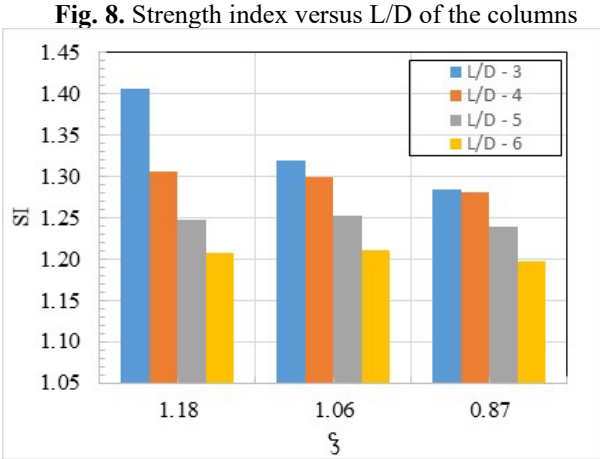

Fig. 9. Strength index versus confinement of the columns

Another important parameter that collaborates with strength index in exploring the column performance is relative slenderness ratio (λ) which is mentioned in Table 1. Fig. 10 shows the performance of SI with relative slenderness ratio. It can be observed that, increment in slenderness reduces the performance of SI. The effect of confinement influenced by the diameter of the column also related in determining the slenderness of the column and its strength index.

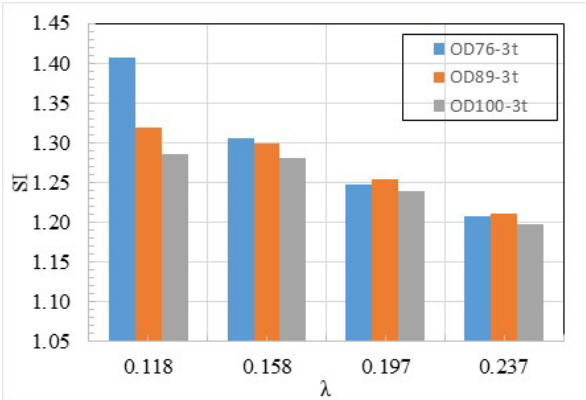

Fig. 10. Strength index versus relative slenderness ratio for all the series of columns

3.5 Percentage Contribution of Steel and Concrete

The contribution of steel (P_s) and concrete (P_c) for all the specimens in the series are analysed by the equations as shown:

$$P_s\ (\%) = \frac{f_y A_s}{N_e} \quad (2)$$

$$P_c\ (\%) = 1 - P_s \quad (3)$$

for all the three series of specimens, the values of P_s and P_c are plotted which can be seen in Fig. 11(a) and (b) respectively. Also, the values are summarized in Table 3. It is observed that contribution of concrete in axial capacities of CFST specimens are around 51 – 58% for series 1, 54 – 57% for series 2 and 57 – 60% for series 3. The increment in axial capacities of the columns enhanced the concrete contribution. Considering the diameter of the specimens, it is observed that, values of P_s are generally low for the specimens with higher diameter that is for series 3 (OD100-3t). The reason here is less confinement of the specimens increases the load carrying capacity which results in less contribution of steel and more contribution of concrete to bear the load. However, as the specimen lengths are increasing, the concrete contribution values are decreasing because, the steel wall permits the specimen to deliver huge scope to support the axial load carrying capacity.

3.6 Ductility Index

It is one such parameter that is analysed by the

deformation of specimen. Generally, Ductility Index (DI) is taken from the load versus axial deformation curves. The deflection of the specimen occurred at its ultimate load and deflection corresponding to the load at the point when it comes back to 85% of its ultimate load are considered to calculate the DI values. The expression is given as follows:

$$\mathrm{DI} = \frac{\delta_{85}}{\delta} \tag{4}$$

where δ_{85} is the displacement occurred at fall of 85% in the ultimate load and δ represents the displacement occurred at ultimate load of the specimen. The ductility index values are calculated as shown in Fig. 12 which is a load versus deformation curve for specimen having ID - OD76-3t in series 1 with L/D ratio of 3. All the DI values for three series with different L/D ratios are compared and represented graphically in Fig. 13. The DI values are higher for the specimens with greater confinement effect, and it is observed a decrement in values for increased L/D ratios in all the series. Compared to series 1 and 2, the specimens in series 3 showed smooth curves till the post peak transition particularly for L/D values 4, 5 and 6.

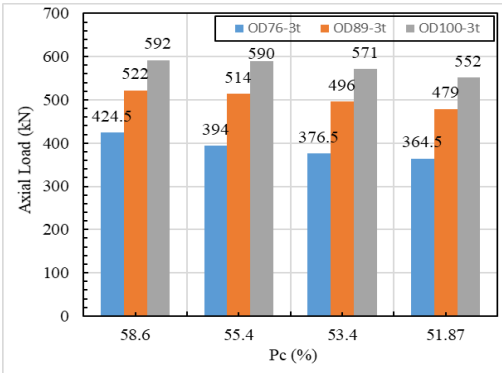

(a) Contribution of steel

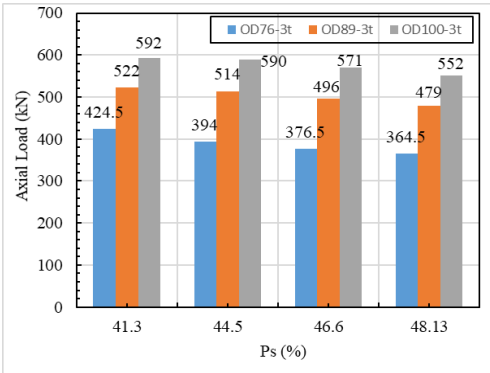

(b) Contribution of concrete

Fig. 11. Contribution of steel and concrete on axial capacities of CFST columns

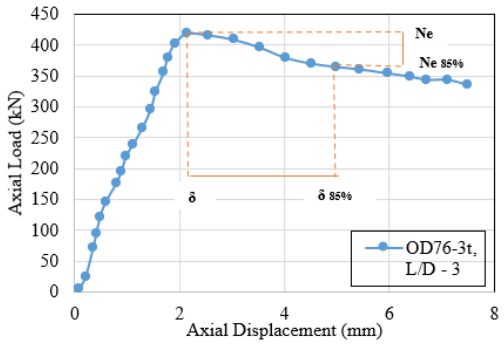

Fig. 12. Calculation of ductility index from load – displacement curve

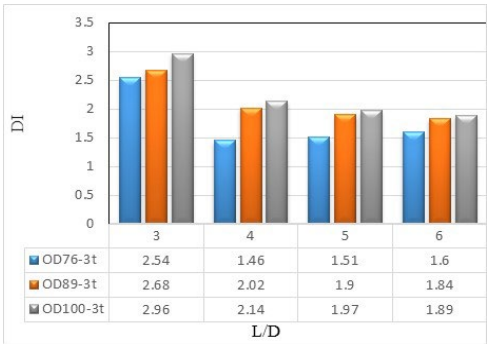

Fig. 13. Ductility index for all the series of specimens

4. CODE PREDICTIONS AND COMPARISON

As the experimental data base on stub CFST columns are less, the design codes that are used regularly have certain limits in choosing the parametric values. The parametric limits and axial capacity predictions of the design codes can be seen in Table 1. This section manifests the precision of axial compressive test results of CFST columns having different diameters and lengths but same wall thickness is compared with the predicted design values. The approach for the CFST column design in this study is established by Eurocode – 4 (EC4), American code (AISC 360 – 10), Australian code (AS5100), Chinese code (DBJ13-51) and American Concrete Institute (ACI – 318). As the part of analysis, since the concrete compressive strength and yield strength of steel tube are known, partial safety factors in the axial capacity prediction equations are taken as unity in all the codes. The predicted axial capacity of different codes is summarized in Table 4 and represented graphically from Figs. 14 to 18.

4.1 Eurocode 4 (EC4)

The axial compressive predicted capacities (N_{EC4}) are shown in Table 4 along with experimental result to predicted result (N_e/N_{EC4}) for all the series and L/D values. EC4 code gives conservative results with a mean, standard deviation

and coefficient of variance (COV) of 1.01, 0.02 and 0.019 respectively. Two specimens, one in series 2 with L/D ratio of 3 and other in series 3 with same L/D ratio showed un-conservative result. Fig. 14 shows L/D versus N_e/N_{EC4} for all the three series of specimens. As L/D of the column increases, axial capacity decreases, however, the predictions of EC4 are very precise and hence showed conservative results.

Table 4. Experimental and code comparisons of CFST axial capacity

Series and Title		N_e kN	EC4		AISC		AS5100		DBJ13-51		ACI		Proposed ACI	
			N_{EC4} (kN)	N_e/N_{EC4}	N_{AISC} (kN)	N_e/N_{AISC}	N_{AS5100} (kN)	N_e/N_{AS5100}	N_{DBJ} (kN)	N_e/N_{DBJ}	N_{ACI} (kN)	N_e/N_{ACI}	P-N_{ACI} (kN)	N_e/ P-N_{ACI}
1	OD76-3t	424	404.5	1.049	314.77	1.349	292.2	1.453	410.5	1.034	297.6	1.426	349.19	1.216
	OD76-3t	394	386.8	1.018	313.38	1.257	284.2	1.386	410.5	0.960	297.6	1.324	340.83	1.156
	OD76-3t	376	371.2	1.014	311.61	1.208	276.6	1.361	410.5	0.971	297.6	1.265	334.58	1.125
	OD76-3t	364	354.7	1.028	309.45	1.178	269.9	1.351	410.5	0.888	297.6	1.224	329.63	1.106
2	OD89-3t	522	528.8	0.987	402.72	1.296	380.46	1.372	534.2	0.977	393.8	1.326	458.38	1.039
	OD89-3t	514	506.2	1.015	400.88	1.282	370.13	1.389	534.2	0.962	393.8	1.305	447.90	1.048
	OD89-3t	496	486.3	1.020	398.54	1.245	360.73	1.375	534.2	0.928	393.8	1.260	440.07	1.127
	OD89-3t	479	469.0	1.021	395.69	1.211	352.25	1.360	534.2	0.897	393.8	1.216	433.86	1.104
3	OD100-3t	592	610.5	0.970	484.4	1.220	435.7	1.359	614.7	0.963	466	1.270	534.48	1.108
	OD100-3t	590	585.8	1.007	482.4	1.230	424.74	1.389	614.7	0.960	466	1.266	523.37	1.027
	OD100-3t	571	564.0	1.012	479.5	1.190	414.72	1.377	614.7	0.929	466	1.225	515.07	1.109
	OD100-3t	552	545.2	1.012	475.9	1.160	405.63	1.361	614.7	0.898	466	1.184	508.49	1.086
		Mean		1.013		1.236		1.378		0.947		1.274		1.097
		SD		0.020		0.054		0.027		0.041		0.064		0.040
		COV		0.019		0.044		0.020		0.044		0.051		0.036

4.2 American Institute of Steel Construction (AISC 360-10)

The predicted values of the CFST specimens (N_{AISC}) and the test to code values (N_e/N_{AISC}) are summarized in Table 4. It is observed that the predicted axial compressive values of AISC 360-10 are lesser than experimental results and hence, N_e/N_{AISC} values are greater than unity which remarks that code gives underestimated results. The mean, standard deviation and COV of the specimens are 1.236, 0.054 and 0.044 respectively. Fig. 15 shows the plot between L/D and N_e/N_{AISC} for all the series of specimens having various L/D ratios. The predicted values vary from 16 – 34% that are lesser than the experimental results with a mean variation around 23%. Therefore, it can be mentioned that AISC 360-10 code gives underestimated results for the CFST specimens in all the three series.

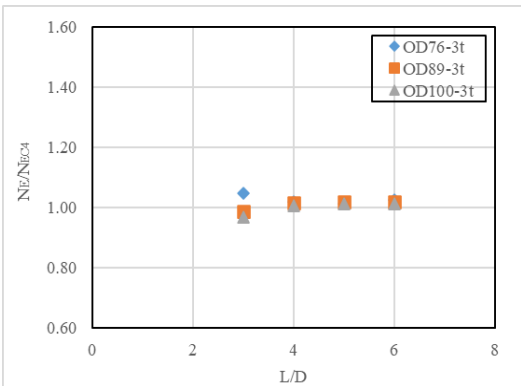

Fig. 14. Comparison of predicted axial capacities to experimental results for various L/D ratios in EC4 code

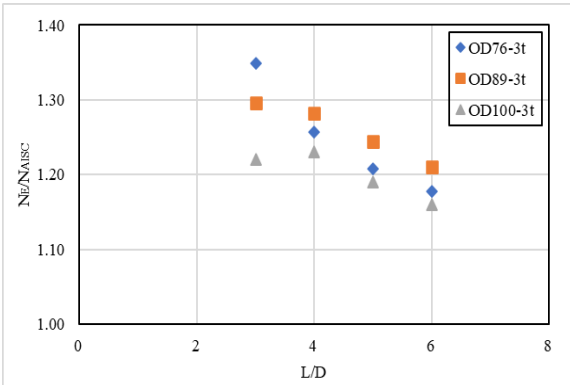

Fig. 15. Comparison of predicted axial capacities to experimental results for various L/D ratios in AISC code

4.3 Australian Standards (AS5100)

The axial compressive capacity calculated from the design code (N_{AS5100}) along with test to code (N_e/N_{AS5100}) for all the series of specimens are listed in Table 4. These predictions are similar to AISC 360 – 10 having greater variation than the experimental results. The mean, standard deviation and COV of the specimens are 1.378, 0.027 and 0.020 respectively. Fig. 16 shows the plot between L/D and N_e/N_{AS5100} for all the series of columns. The axial predicted capacities are around 35 – 38% lesser than the experimental results while one specimen in series 1 (OD76-3t) having L/D of 3 showed 45% lesser value than the experimental result. The mean variation of the predicted results of the CFST specimens are around 37% lesser than the test results which confirm that, AS5100 showed underestimated results in predicting the column capacity.

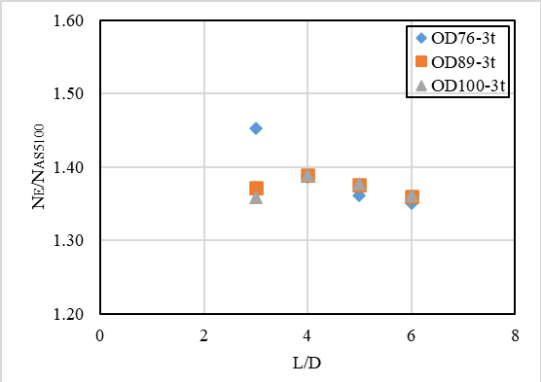

Fig. 16. Comparison of predicted axial capacities to experimental results for various L/D ratios in AS5100 code

4.4 Chinese Code (DBJ13-51)

The design predicted values (N_{DBJ}) and test to code values (N_e/N_{DBJ}) are listed in Table 4 and the graphical representation for L/D versus N_e/N_{DBJ} for all the specimens in the series is seen in Fig. 17. The mean, standard deviation and COV of the specimens in all the series having 0.947, 0.041 and 0.44 respectively shows over-conservative results in predicting the column capacity. All the specimens in the series show 3 – 12% higher values than the experimental results while one specimen in series 1 (OD76-3t) with L/D ratio 3 showed conservative result with N_e/N_{DBJ} value of 1.034. The mean value of all the specimens being 0.947, code DBJ13-51 shows overestimated results.

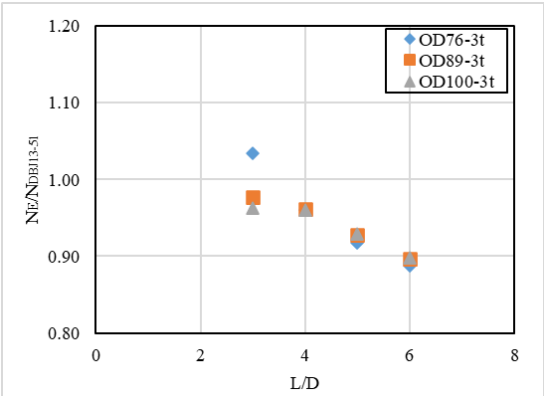

Fig. 17. Comparison of predicted axial capacities to experimental results for various L/D ratios in DBJ13-51 code

4.5 American Concrete Institute (ACI – 318)

The axial load predicted values from the code (N_{ACI}) and the test to code (N_e/N_{ACI}) are listed in Table 4. The mean, standard deviation and COV of the specimens are 1.274, 0.064 and 0.051 respectively. It can be observed that the predicted values are around 18 – 42% lesser than the experimental results and hence the N_e/N_{ACI} values are greater than unity and are un-conservative. Fig. 18 shows the graph plotted between L/D and N_e/N_{ACI} for all the specimens.

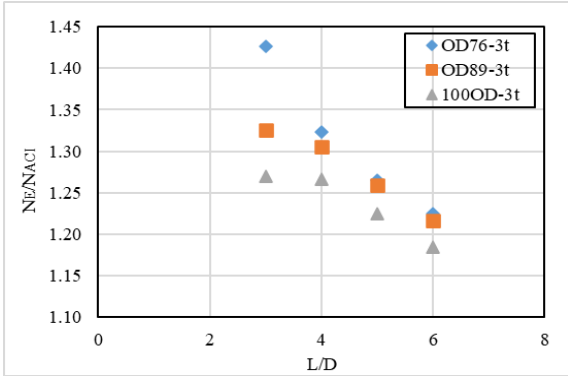

Fig. 18. Comparison of predicted axial capacities to experimental results for various L/D ratios in code ACI – 318

5. PROPOSED EQUATION PREDICTIONS AND COMPARISONS

On the basis of experimental test results, a factor 'k' is arrived in terms of L/D ratio. From the graph plotted between k versus L/D, a best fitting curve is adopted that can predict the ultimate axial load of the CFST column irrespective of the diameter.

$$P - N_{ACI} = k[0.85 f_c A_c + f_y A_s] \quad (5)$$
$$k = 1.583\,(L/D)^{-0.148}$$

The proposed Equation (5) is compared with the experimental test results. Table 4 shows the test to proposed equation results (N_e/P-N_{ACI}) having mean, standard deviation and COV of 1.097, 0.040 and 0.036 respectively. This shows the proposed equation predicted the results very near to the experimental test results and hence, the proposed equation gave conservative results. Fig. 19 shows the comparison of N_e versus N_{ACI} and N_e versus P-N_{ACI}. It can be seen that all the points in P-N_{ACI} fall in a straight line with R^2 value being 0.98 while the points of N_{ACI} having R^2 value of 0.9023.

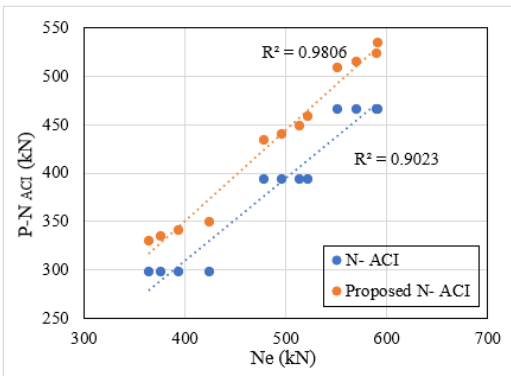

Fig. 19. Comparison of experimental test results with ACI and proposed ACI

Further, to check the accuracy of the proposed equation, comparison is done with the experimental test results obtained from the literatures. Table 5 shows the experimental test results of 63 CFST specimens from references Wang et al. (2017), Li et al. (2020) and Ahamed et al. (2020) that are compared with EC4, AS5100, DBJ13-51, ACI – 318 and Proposed N- ACI. The mean of EC4 predictions is 1.079 which shows conservative results while AS5100 and ACI – 318 codes having the mean value of 1.648 and 1.398 respectively which are unconservative. DBJ13-51 gives the mean value of 1.179 which is again unconservative by 17%.

However, the proposed N- ACI gives the mean, standard deviation and COV of 1.097, 0.096 and 0.094 respectively. Hence, it is inferred here that the predictions of proposed equation are very near to accuracy and shows conservative results. It is reminded here that the agreement of axial load test results is not end in itself, but in this case, the Equation (5) proved the accuracy in determining the axial capacity.

Table 5. Comparison of literature experimental results to predicted results

Ref.	N_e (kN)	EC4		AS5100		DBJ13-51		ACI		Proposed ACI	
		N_{EC4} (kN)	N_e/N_{EC4}	N_{AS5100} (kN)	N_e/N_{AS5100}	N_{DBJ} (kN)	N_e/N_{DBJ}	N_{ACI} (kN)	N_e/N_{ACI}	P-N_{ACI} (kN)	N_e/P-N_{ACI}
Wang et al. (2017)	4234	5625.37	0.753	2253.85	1.879	2537.52	1.669	2602.11	1.627	3661.33	1.156
	4245	5597.36	0.758	2275.44	1.866	2561.30	1.657	2628.80	1.615	3703.61	1.146
	14469	19673.56	0.735	7377.56	1.961	8549.77	1.692	8966.06	1.614	12605.71	1.148
	15077	21015.25	0.717	7513.73	2.007	8693.08	1.734	9071.60	1.662	12759.92	1.182
	29463	38450.81	0.766	15591.29	1.890	18157.59	1.623	19168.94	1.537	26926.97	1.094
	29294	38043.40	0.770	15578.79	1.880	18143.08	1.615	19152.41	1.530	26900.96	1.089
	3364	3254.91	1.034	2054.02	1.638	2308.63	1.457	2958.72	1.137	4148.66	0.811
	4244	5138.50	0.826	2479.45	1.712	2786.62	1.523	2982.65	1.423	4186.39	1.014
	12360	14392.45	0.859	7070.37	1.748	8642.08	1.430	9640.69	1.282	13565.20	0.911
	13092	16225.88	0.807	7038.04	1.860	8602.06	1.522	9593.82	1.365	13491.73	0.970
	23663	24414.61	0.969	15309.76	1.546	18646.53	1.269	20820.91	1.137	29240.46	0.809
	26002	29077.60	0.894	15480.14	1.680	18889.12	1.377	21162.57	1.229	29786.71	0.873
Li et al. (2020)	1260	1241.81	1.015	868.20	1.451	1294.62	0.973	1045.37	1.205	1437.23	0.877
	1660	1469.23	1.130	1051.53	1.579	1504.62	1.103	1175.77	1.412	1616.52	1.027
	1785	1602.47	1.114	1157.16	1.543	1639.08	1.089	1250.94	1.427	1719.87	1.038
	1390	1396.64	0.995	966.96	1.438	1494.06	0.930	1208.84	1.150	1661.99	0.836
	1690	1565.82	1.079	1105.24	1.529	1659.95	1.018	1301.36	1.299	1789.19	0.945
	1890	1751.96	1.079	1256.03	1.505	1843.43	1.025	1410.26	1.340	1938.92	0.975
	1450	1508.21	0.961	1037.73	1.397	1637.10	0.886	1326.09	1.093	1823.18	0.795
	1789	1724.12	1.038	1216.76	1.470	1847.09	0.969	1448.80	1.235	1991.90	0.898
	1990	1850.17	1.076	1319.04	1.509	1981.55	1.004	1518.28	1.311	2087.42	0.953
	1600	1279.25	1.251	898.66	1.780	1326.73	1.206	1070.53	1.495	1471.83	1.087
	1900	1472.21	1.291	1053.48	1.804	1508.65	1.259	1178.98	1.612	1620.93	1.172
	1960	1605.37	1.221	1159.07	1.691	1643.11	1.193	1254.09	1.563	1724.20	1.137
	1690	1379.39	1.225	955.99	1.768	1471.90	1.148	1190.68	1.419	1637.02	1.032
	1990	1600.84	1.243	1137.10	1.750	1681.90	1.183	1317.10	1.511	1810.83	1.099
	2020	1730.37	1.167	1241.00	1.628	1816.36	1.112	1389.33	1.454	1910.13	1.058
	1850	1495.62	1.237	1029.76	1.797	1620.98	1.141	1312.88	1.409	1805.02	1.025
	2185	1712.07	1.276	1208.99	1.807	1830.97	1.193	1435.95	1.522	1974.23	1.107
	2397	1838.47	1.304	1311.43	1.828	1965.44	1.220	1505.70	1.592	2070.12	1.158
	1700	1369.99	1.241	950.01	1.789	1459.82	1.165	1180.77	1.440	1623.40	1.047
	1990	1591.84	1.250	1131.27	1.759	1669.81	1.192	1307.47	1.522	1797.58	1.107
	2135	1721.63	1.240	1235.29	1.728	1804.27	1.183	1379.89	1.547	1897.16	1.125
	1890	1602.80	1.179	1097.51	1.722	1757.97	1.075	1425.17	1.326	1959.40	0.965
	2100	1814.69	1.157	1275.01	1.647	1967.96	1.067	1545.16	1.359	2124.38	0.989
	2230	1938.19	1.151	1376.11	1.621	2102.42	1.061	1612.63	1.383	2217.14	1.006
	1940	1621.75	1.196	1109.46	1.749	1782.15	1.089	1444.98	1.343	1986.65	0.977
	2100	1832.83	1.146	1286.65	1.632	1992.14	1.054	1564.44	1.342	2150.88	0.976
	2250	1955.83	1.150	1387.52	1.622	2126.60	1.058	1631.50	1.379	2243.08	1.003
	1625	1343.36	1.210	933.05	1.742	1425.57	1.140	1152.70	1.410	1584.80	1.025
	1950	1566.37	1.245	1114.75	1.749	1635.56	1.192	1280.16	1.523	1760.04	1.108
	2010	1696.87	1.185	1219.10	1.649	1770.02	1.136	1353.16	1.485	1860.40	1.080
	1880	1387.23	1.355	960.98	1.956	1481.98	1.269	1198.94	1.568	1648.37	1.141
	2140	1608.34	1.331	1141.96	1.874	1691.97	1.265	1325.13	1.615	1821.87	1.175
	2200	1737.66	1.266	1245.77	1.766	1826.43	1.205	1397.19	1.575	1920.94	1.145
	1700	1476.75	1.151	1017.80	1.670	1596.81	1.065	1293.06	1.315	1777.78	0.956

	1950	1694.01	1.151	1197.34	1.629	1806.80	1.079	1416.68	1.376	1947.73	1.001
	2080	1820.91	1.142	1300.02	1.600	1941.26	1.071	1486.83	1.399	2044.18	1.018
	345	339.45	1.016	241.40	1.429	321.23	1.074	251.93	1.369	357.74	0.964
	351	339.45	1.034	241.40	1.454	321.23	1.093	251.93	1.393	357.74	0.981
	376	359.47	1.046	254.35	1.478	347.92	1.081	273.34	1.376	388.15	0.969
	355	359.47	0.988	254.35	1.396	347.92	1.020	273.34	1.299	388.15	0.915
	396	390.54	1.014	274.35	1.443	389.15	1.018	306.42	1.292	435.12	0.910
	415	390.54	1.063	274.35	1.513	389.15	1.066	306.42	1.354	435.12	0.954
Ahmad	435	391.67	1.111	275.07	1.581	390.65	1.114	307.62	1.414	436.82	0.996
et al.	424	391.67	1.083	275.07	1.541	390.65	1.085	307.62	1.378	436.82	0.971
(2020)	325	323.67	1.004	234.39	1.387	321.23	1.012	251.93	1.290	332.66	0.977
	340	323.67	1.050	234.39	1.451	321.23	1.058	251.93	1.350	332.66	1.022
	350	343.38	1.019	247.38	1.415	347.92	1.006	273.34	1.280	360.94	0.970
	380	373.99	1.016	267.42	1.421	389.15	0.976	306.42	1.240	404.62	0.939
	400	373.99	1.070	267.42	1.496	389.15	1.028	306.42	1.305	404.62	0.989
	410	375.11	1.093	268.14	1.529	390.65	1.050	307.62	1.333	406.20	1.009
	390	375.11	1.040	268.14	1.454	390.65	0.998	307.62	1.268	406.20	0.960
		Mean	1.079		1.648		1.179		1.398		1.013
		SD	0.160		0.165		0.205		0.135		0.096
		COV	0.148		0.100		0.174		0.096		0.094

6. FE MODELLING OF CFST WITH ABAQUS

Abaqus/CAE – 6.14 tool was used to develop the model of all 24 CFST specimens subjecting to axial loading. Buckling of columns, failure modes and axial load versus deformation curves were generated through FE modelling and compared with experimental test results. Deformable and homogeneous element shell was used in modelling and developing the steel tube. While, deformable and solid element was used for concrete core.

Material properties of steel and concrete in the tool were defined as same as the experimental test results. 'Full Newton' estimation was selected to run the program using nonlinear geometry solvers. Only axial deformation along the length of the specimen was permitted in boundary condition. Formation of reference points at the ends of column was confirmed to concentric loading, fixed end boundary condition was applied to all the specimens and to reduce the variation of mesh conversion, a structured type of mesh control was used.

In the procedure of CFST modelling, displacement was applied in vertical direction. Load versus displacement curves for all the columns were generated after the analysis. The best comparisons of experimental and FE test results are seen for columns having L/D of 4 and is shown in Fig. 20. Experimental and FE axial test results of all the CFST specimens are listed in Table 6. FEA results showed a difference of 6 - 10% from experimental results. However, few specimens (OD89-3t-5, OD100-3t-6) exhibited 19% difference which identified few geometrical imperfections.

Fig. 21 shows the comparison of deformed shapes of FE models and experimental failure specimens. All the specimens showed outward local bucking.

7. CONCLUSIONS

The effect of confinement due to outer diameter and effect of axial capacity due to various L/D ratios (3,4,5,6) and ductility were studied for all the 24 CFST specimens. Then, design code predictions on axial capacities were compared to the experimental results. Based on this, design equation is proposed for determining the ultimate axial capacities. The conclusions are drawn below.

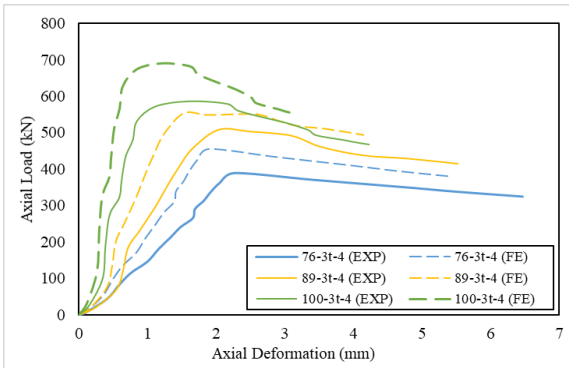

Fig. 20. Axial load versus axial deformation curves of experimental and FE CFST columns

Local buckling mode of failure is observed in all the CFST specimens. Less ductility is seen in the columns having outer diameter of 76 mm with L/D ratio of 3. The strength index (SI) of the CFST specimens can be increased with increasing the effect of confinement (ξ). However, the axial capacities are decreased with increasing the slenderness of the column.

The experimental study fulfilled the statement that using greater outer diameter steel tubes immensely increased the concrete contribution ratio with increasing L/D.

The axial design capacities were evaluated by the standard codes: EC4, AISC 360 – 10, AS5100, DBJ13-51

and ACI-318. Correlation showed that EC4 gives greater traditional outcomes. AISC 360 – 10 and AS5100 showed underestimated results, which is similar in ACI – 318 as well. DBJ13 – 51 showed overestimated results as the fact being that the parameter L/D has no significance in the design procedure of column in the code.

The predicted ultimate axial load results obtained from the proposed equation agreed well with the experimental test results as well as with the experimental results from the literature.

FE models using ABAQUS for all the CFST specimens were developed in this study. Good agreement is observed in axial test results, buckling pattern and axial deformation curves for both experimental and FE model's output.

Table 6. Experimental and FEA model comparisons of CFST axial capacity

Series	Title	L/D	N_e (kN)	FEA (kN)	
				N_{FEA} (kN)	N_e/N_{FEA}
1	OD76-3t	3	424.5	440.14	0.964
	OD76-3t	4	394	417.73	0.943
	OD76-3t	5	376.5	378.37	0.995
	OD76-3t	6	364.5	375	0.972
2	OD89-3t	3	522	578.14	0.903
	OD89-3t	4	514	554.61	0.927
	OD89-3t	5	496	593.42	0.836
	OD89-3t	6	479	517.05	0.926
3	OD100-3t	3	592	683.05	0.867
	OD100-3t	4	590	690.31	0.855
	OD100-3t	5	571	665.57	0.858
	OD100-3t	6	552	657.08	0.840
				Mean	0.970
				SD	0.053
				COV	0.058

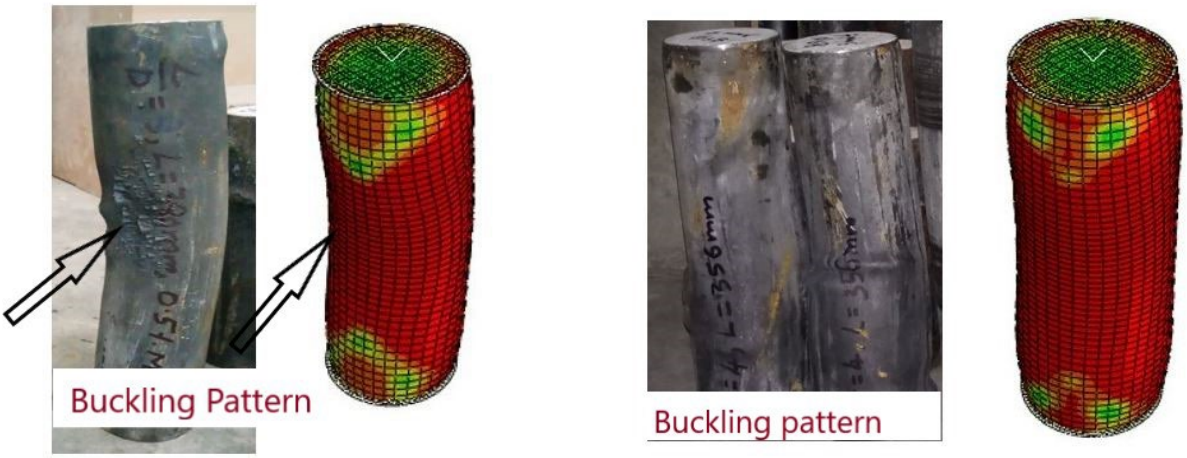

Fig. 21. Bucking patterns of CFST columns in ABAQUS and tested specimens

REFERENCES

Abed, F., Alhamaydeh, M., Abdalla, S. 2013. Experimental and numerical investigations of the compressive behavior of concrete filled steel tubes (CFSTs). Journal of Constructional Steel Research, 80, 429–439.

Ahmad, S., Kumar, A., Kumar, K. 2020. Axial performance of GGBFS concrete filled steel tubes. Structures, 23, 539–550.

AS 5100.6-2004. Bridge Design part 6: steel and composite construction. AS. Sydney.

Beck, A.T., de Oliveira, W.L.A., De Nardim, S., El Debs, A.L.H.C. 2009. Reliability-based evaluation of design

code provisions for circular concrete-filled steel columns. Engineering Structures, 31, 2299–2308.

Chen, C., Wang, C., Sun, H. 2014. Experimental study on seismic behavior of full encased steel-concrete composite columns. Journal of Structural Engineering, 140, 4024-4034.

Chitawadagi, M.V., Narasimhan, M.C., Kulkarni, S.M. 2010. Axial strength of circular concrete-filled steel tube columns - DOE approach. Journal of Constructional Steel Research, 66, 1248–1260.

Dar, M.A., Subramanian, N., Anbarasu, M., Ghowsi, A.F, Arif, P.A., Dar, A.R. 2021. Testing and FE simulation of lightweight CFS composite built-up columns: Axial strength and deformation behaviour. Thin-Walled Structures, 167, 108222.

Dundu, M. 2012. Compressive strength of circular concrete filled steel tube columns. Thin Walled Structures, 56, 62–70.

Ekmekyapar, T., Al-Eliwi, B. J. M. 2016. Experimental behaviour of circular concrete filled steel tube columns and design specifications. Thin Walled Structures, 220–230.

EN 1994-1-1 Eurocode 4. Design of composite steel and concrete structures – part 1-1: General rules and rules for buildings. CEN. Brussels.

Evirgen, B., Tuncan, A., Taskin, K. 2014. Structural behavior of concrete filled steel tubular sections (CFT/CFSt) under axial compression. Thin Walled Structures, 80, 46–56.

Fang, H., Visintin, P. 2021. Structural performance of geopolymer-concrete filled steel tube members subjected to compression and bending. Journal of Constructional Steel Research, 188, 107026.

Feng, Y., Chen, L., Shuangshuang, B., Huang, W., Yuan, F. 2020. Experimental and theoretical investigations of recycled self-compacting concrete filled steel tubular columns subjected to axial compression. Construction and Building Materials, 248, 689–706.

Giakoumelis, G., Lam, D. 2004. Axial capacity of circular concrete-filled tube columns. Journal of Constructional Steel Research, 60, 1049–1068.

Han, L.H. 2002. Tests on stub columns of concrete filled RHS sections. Journal of constructional steel research, 58, 353–372.

Han, L.H., Yao, G.H., Zhao, X.L. 2005. Tests and calculations for hollow structural steel (HSS) stub columns filled with self-consolidating concrete (SCC). Journal of Constructional Steel Research, 61, 1241–1269.

Hu, H.T., Huang, C.S., Wu, M.H., Wu, Y.M. 2003. Nonlinear analysis of axially loaded concrete-filled tube columns with confinement effect. Journal of Structural Engineering, 129, 1322–1329.

Idris, Y., Ozbakkaloglu, T. 2013. Seismic behavior of high-strength concrete-filled FRP tube columns. Journal of Composites for Construction, 17, 3013–3026.

Kato, B. 1996. Column Curves of Steel-Concrete Composite Members. Journal of Constructional Steel Research, 39, 121–135.

Kazemzadeh, A.S., Brian, U. 2020. Effect of concrete infill on local buckling capacity of circular tubes. Journal of Constructional Steel Research, 165, 899-921.

Li, N., Lu, Y., Li, S., Gao, D. 2020. Axial compressive behaviour of steel fibre reinforced self-stressing and self-compacting concrete-filled steel tube columns. Engineering Structures, 222, 108–120.

Liang, W., Dong, J.F., Yuan, S.C., Wang., Q.Y. 2017. Behavior of self-compacting concrete-filled steel tube columns with inclined stiffener ribs under axial compression. Strength of Materials, 49, 125–132.

Liu, D., Gho, W.M. 2005. Axial load behaviour of high-strength rectangular concrete-filled steel tubular stub columns. Thin Walled Structures, 43, 1131–1142.

Liu, Z., Lu, Y., Li, S. Yi, S. 2019. Behavior of steel tube columns filled with steel-fiber-reinforced self-stressing recycled aggregate concrete under axial compression. Thin Walled Structures, 149, 521–529.

Lu, Y., Zhenzhen, L., Shan, L., Xiaobo, Z. 2019. Effect of the outer diameter on the behavior of square RC columns strengthened with self-compacting concrete filled circular steel tube. International Journal of Steel Structures, 19, 1042–1054.

Ou, Z., Chen, B., Hsieh, K.H., Halling, M.W., Barr, P.J. 2011. Experimental and analytical investigation of concrete filled steel tubular columns. Journal of Structural Engineering, 137, 635–645.

Sakino, K., Nakahara, H., Morino, S., Nishiyama, I. 2004. Behavior of centrally loaded concrete-filled steel-tube short columns. Journal of Structural Engineering, 130, 180–188.

Shanmugam, N.E., Lakshmi, B. 2001. State of the art report on steel – concrete composite columns. Journal of Constructional Steel Research, 57, 1041–1080.

Wang, W., Ma, H., Li, Z., Tang, Z. 2017. Size effect in circular concrete-filled steel tubes with different diameter-to-thickness ratios under axial compression. Engineering Structures, 151, 554–567.

Wang, Y., Ligui, Y., Yang, H., Changyong, L. 2019. Behaviour of concrete-filled corrugated steel tubes under axial compression. Engineering Structures, 18, 475–95.

Wu, Y.Z., Xing, D.F., Cai, C.S. 2007. Experimental behavior of circular concrete-filled steel tube stub columns. Journal of Constructional Steel Research, 63, 165–174.

Xiao, Y., He, W., Choi, K.K. 2005. Confined concrete-filled tubular columns. Journal of Structural Engineering, 131, 488–497.

Yu, M., Zha, X., Ye, J., She, C. 2010. A unified formulation for hollow and solid concrete filled steel tube columns under axial compression. Engineering Structures, 32, 1046-1053.

Zeghiche. J., Chaoui, K. 2005. An experimental behaviour of concrete-filled steel tubular columns. Journal of Constructional Steel Research, 61, 53–66.

Zhao, X.L., Han, L.H., Lu, H. 2010. Concrete filled tubular members and connections. Spon press. London.

Zhao, H.L., Zhao, Y., Ying, C.J. 2018. A simple formula for predicting the compressive strength of circular CFT stub columns. Journal of Asian Architecture and Building Engineering, 8, 167–173.

Zhou, S., Qing, S., Xiaohong, W. 2018. Impact of d/t ratio on circular concrete-filled high-strength steel tubular stub columns under axial compression. Thin Walled Structures, 132, 461–474.